Simultaneous Clock and RF Carrier Distribution for Beyond 5G Networks Using Optical Frequency Comb

Zichuan Zhou, Dhecha Nopchinda, Mu-Chieh Lo, Izzat Darwazeh and Zhixin Liu

Department of Electronic and Electrical Engineering, University College London, zczlzz0@ucl.ac.uk

Abstract *We demonstrate sub-100fs jitter, dispersion-tolerant dissemination of 5-GHz-spaced RF tones up to 45GHz using a filtered optical frequency comb, enabling clock and RF carrier synchronised wireless communication systems with 1.4Gb/s data rate. The impact of seed laser linewidth on RF phase noise is also studied. ©2022 The Author(s)*

Introduction

The massive multiple-input multiple-output (MIMO), distributed antenna systems and ultra-dense cells in 5G/6G wireless networks require synchronized clock and radio frequency (RF) carriers between different radio units (RU, e.g., base stations) to enable accurate positioning and ultra-reliable low-latency communications [1-4]. Furthermore, RUs and wireless devices must be able to access multiple RF bands for wireless communications. For example, 5G systems specify both sub-6 GHz and 28 GHz carriers for data transmission. Beyond that, emerging 6G research proposes to operate in multiple bands over a wide frequency region [5,6].

This has motivated radio-over-fibre (RoF) research that transmits RF signals through low-loss optical fibres from central offices to RUs to generate synchronised RF signals using broadband photodetectors [7-10]. Optical frequency combs that generate coherent and equally spaced optical tones can provide multiple equally spaced RF tones [11-13], i.e., an RF comb, offering a promising way to generate synchronised RF tones over a wide bandwidth as the carriers and local oscillators (LO) for different RF bands, as conceptually shown in Fig.1.

Nevertheless, the RF tones generated by direct detecting transmitted optical frequency combs suffer from the dispersion-induced frequency fading and a relatively poor jitter due to the decoherence of the optical tones after transmission [14-17]. Furthermore, the RoF demonstrations so far primarily focus on RF signal transmission, whilst the clock of radio access networks (RAN) is distributed using the synchronous ethernet (Sync-E) approach [18,19], which extracts clock components from modulated data packets, resulting in a poor jitter value of 10s of ps [18,19], limiting the digitization' accuracy for high spectral-efficiency signals [20].

In this paper, we overcome the above-mentioned challenges by proposing and demonstrating simultaneous clock and RF signal distribution using a filtered opto-electronic frequency comb, resulting in <100 fs jitter clock (integrated from 1 kHz to 10 MHz) and low-noise RF tones from 5 GHz to 45 GHz (limited by the photodetector) with 5 GHz spacing. The filtered single-side band optical frequency comb has a strong tolerance to dispersion and showed similar RF power in each tone at various fibre length up to 22 km. We further conduct a proof-of-concept wireless transmission experiment using the distributed clock and RF signals as the reference clock and RF carriers, demonstrating up to 1.4 Gb/s wireless data transmission using 200 MBaud 64 QAM and 128 QAM formats.

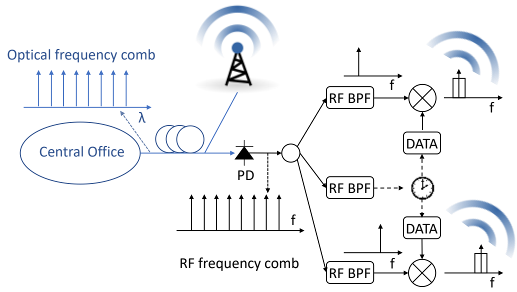

Fig.1 conceptual diagram of the proposed system.

Experimental Set-up

Fig. 2a shows our experimental set-up comprising an optical frequency comb dissemination system in blue and the wireless transmission systems in grey. A continuous wave (CW) laser seeds an opto-electronic frequency comb generator consisting of a phase modulator (PM) followed by a Mach-Zehnder modulator (MZM) driven by a 5 GHz RF signal [13], yielding a 5-GHz-spaced optical frequency comb with a spectral flatness of about 6 dB. Three CW lasers of different linewidth (100 kHz, 5 kHz and 100 Hz) emitting at 1555 nm are used to study the degradation of phase noise after transmission. We subsequently amplified the comb signals using an erbium-doped fibre amplifier (EDFA) from 0 dBm to 19 dBm and filtered the lower side band of the comb signals

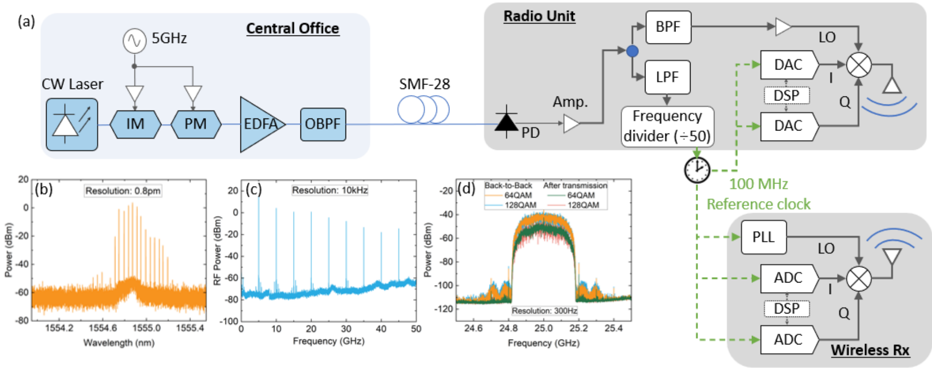

Fig. 2: (a) Experimental set-up. OBPF: optical bandpass filter, PD: photodetector, PLL: phase-locked-loop, DSP: digital signal processing (b) Optical spectrum of filtered optical frequency comb, (c) Electrical spectrum of RF frequency comb at 3.5 dBm received optical power, (d) Electrical spectrum of RF 64/128QAM signal

using a bandpass filter. The optical spectra of the frequency combs are shown in Fig. 2b. The filtered comb signals are transmitted through standard single mode fibres (SMF-28) to the RU side before detection by a 50Ω-coupled 40 GHz photodetector. Different fibre lengths (6, 10, 16 and 22km) were used to evaluate the dispersion tolerance of the transmitted RF signals. The coherent optical tones beat with each other and generate an RF comb signal with 5 GHz spacing, which is amplified by 40 GHz RF amplifier with 38 dB gain. The spectrum of the disseminated RF signal is shown in Fig. 2c, where the 5 GHz RF tone has the highest power and the power decreases for the high frequency tones due to reduced number of optical tone pairs with a larger frequency spacing as well as the frequency roll-off of the photodetector.

At the RU side, the RF signals are split by a 1×2 Wilkinson RF power splitter, with one branch connected to a 5.5 GHz bandwidth low pass filter (LPF) to extract the 5 GHz RF signals, which is subsequently divided to 100 MHz as the reference clock for the wireless systems (shown as the dashed line in Fig. 2a).

The other output of the splitter is connected to a 50 MHz bandwidth RF bandpass filter (BPF) centred at 25 GHz to extract the 25 GHz RF tone as the local oscillator of the wireless transmitter. Two 16-bit digital to analog converters (DAC) are used to generate the in-phase and quadrature components of 200 MSymbol/s baseband signals using 64 and 128 QAM modulation and digital root-raised cosine pulse shaping with a 0.8 roll-off factor. The generated I and Q signals modulate the 25 GHz 20 dBm LO through an IQ mixer, generating modulated RF signals with a net data rate 1.2 Gb/s and 1.4 Gb/s, using 64 QAM and 128 QAM, respectively. Fig. 2d shows the corresponding spectrum. The RF is transmitted using a horn antenna. Another horn antenna was located 10 cm away to receive the wireless signals and down convert to baseband before the IQ components are captured by a two analog to digital converters (ADC) followed by digital signal processing and demodulation, including IQ orthogonalization, match filtering and equalization.

Results and Discussion

We show the dispersion tolerance of our approach in Fig. 3. The markers show the experimental results at different fibre lengths and the dashed curves show the simulation results, using 5 GHz, 25 GHz, and 40 GHz as example. As comparison, we simulate the transmission of an unfiltered frequency comb and show the power fading using dotted curves. Similar to the frequency fading issue in intensity modulation direct detection systems, fibre dispersion causes opposite phase of comb tones in the upper and lower side bands and consequently a significant power fading after transmission. This frequency fading is mitigated by filtering out half of comb lines, resulting in a power change of a few dB without a complete diminishing of the RF power, essential for RF signal distribution [14-17]. The discrepancy in the simulation and experimental

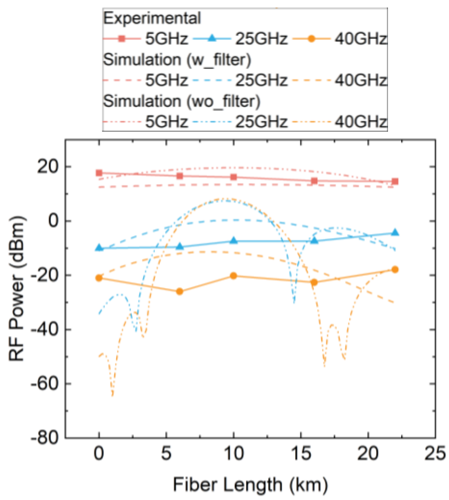

Fig. 3: Distributed RF power after transmitting over different fibre lengths.

results are due to the inaccurate estimation of the fibre dispersion and the spectral shape of the filtered comb.

Fig. 4 shows the measured phase noise of the 25 GHz RF tone at back-to-back (solid curves) and after 22 km SMF-28 transmission (dashed curve) using different seed lasers. All three lasers achieved similar phase noise performance at back-to-back, showing about 82 fs integrated jitter (1kHz to 10MHz). After transmission, the fibre dispersion introduces group velocity difference to the 25-GHz-spacing optical tones pairs and consequently, leading to enhanced phase noise in the low frequency region, resulting in an integrated jitter of 87 fs, 108 fs and 104 fs, respectively for the 100 Hz, 5 kHz and 100 kHz linewidth lasers. Note that the linewidth used here only describes the short-term laser frequency noise, i.e., the Schawlow–Townes linewidth. As the degraded phase noise is primarily in the low frequency region, the low frequency flicker and random walk should be attributed to the increased jitter. The 5-kHz laser used in this work is a fibre laser with a strong 1/f frequency noise which leads to a higher jitter after transmission.

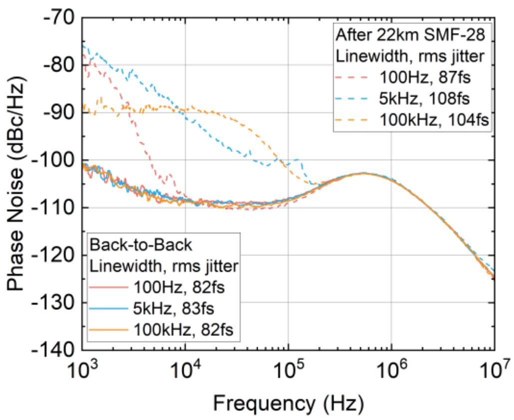

Fig. 4: Phase noise measurement of the detected 25 GHz RF tone using lasers of different linewidth as the seed (a): Back-to-Back, (b): after 22 km SMF-28

Fig. 5 shows error vector magnitude (EVM) of the received wireless signals at different RF power. A back-to-back comparison is made by directly connecting the transmitted RF signals to the receiver's RF input. EVM values of 3.1% and 6.2% are achieved for 64QAM and 128QAM signals, respectively, as shown in the inset constellation diagrams in Fig. 5. After wireless transmission, the EVM results are 7.5% and 8.0%, respectively, for 64QAM and 128QAM signals. The EVM penalty is caused by the limited bandwidth of horn antenna. At -50 dBm received power (i.e., 30 dB loss), we can still achieve EVM values of 13% and 10% for 64QAM and 128QAM after transmission. That means, we could transmit 25 GHz centered wireless signal up to 3 meters, assuming an ideal free-space path loss, 2x20 dBi horns and perfect coupling/alignment.

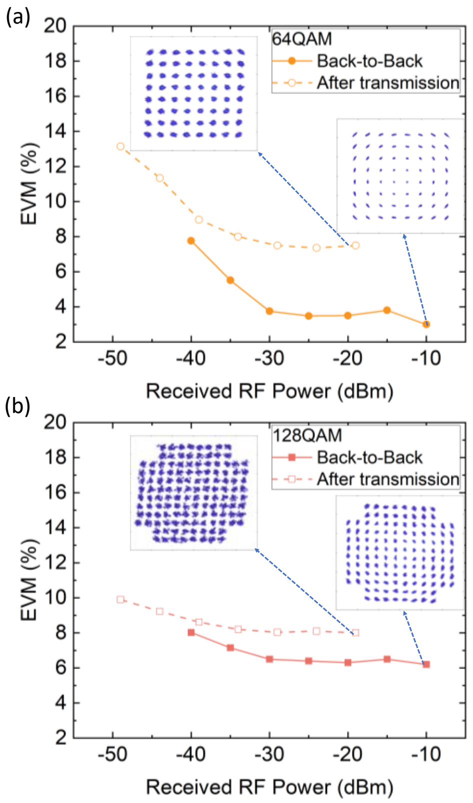

Fig. 5: EVM results at different received RF power (a): 64QAM, (b): 128QAM

Conclusions

We demonstrate simultaneous distribution of sub-100-fs jitter clock and low noise 5-GHz-spaced RF tones using a filtered electro-optic frequency comb, featuring a significantly enhanced tolerance to power fading with less than 10dB RF power variation. By comparing the obtained phase noise using lasers of different linewidth, we show that the decoherence of optical tones mainly degrades the low frequency phase noise. High performance wireless transmission of up to 1.4 Gb/s net rate was achieved using the distributed carrier and clock.

Acknowledgements

The authors acknowledge Royal Society (PIF/R1/180001), EPSRC (EP/R035342/1, EP/R041792/1), European Union's Horizon 2020 research and innovation programme for the funding support (101032236). Dr. D. Nopchinda is funded by the Leverhulme Trust.

References

[1] Z. Jiang et al., “Phase-Stabilized Side-Branch RoF Link for Extensible Frequency Dissemination in Distributed Systems,” in IEEE Photonics Journal, vol. 13, no. 5, pp. 1-7, Oct. 2021, Art no. 7100107, doi: 10.1109/JPHOT.2021.3113663.

[2] M. Sung et al., "Demonstration of IFoF-Based Mobile Fronthaul in 5G Prototype With 28-GHz Millimeter wave," in Journal of Lightwave Technology, vol. 36, no. 2, pp. 601-609, 15 Jan.15, 2018, doi: 10.1109/JLT.2017.2763156.

[3] H. Li et al., “Analysis of the Synchronization Requirements of 5g and Corresponding Solutions,” in IEEE Communications Standards Magazine, vol. 1, no. 1, pp. 52-58, March 2017, doi: 10.1109/MCOMSTD.2017.1600768ST.

[4] M. Koivisto et al., “Joint Device Positioning and Clock Synchronization in 5G Ultra-Dense Networks,” in IEEE Transactions on Wireless Communications, vol. 16, no. 5, pp. 2866-2881, May 2017, doi: 10.1109/TWC.2017.2669963.

[5] “5G spectrum-public policy position”, GSM Association, Nov. 2016.

[6] M. Matinmikko-Blue, S. Yrjölä and P. Ahokangas, “Spectrum Management in the 6G Era: The Role of Regulation and Spectrum Sharing,” 2020 2nd 6G Wireless Summit (6G SUMMIT), 2020, pp. 1-5, doi: 10.1109/6GSUMMIT49458.2020.9083851.

[7] J. Capmany and D. Novak, "Microwave photonics combines two worlds", Nature Photon., vol. 1, pp. 319-330, 2007.DOI: 10.1038/nphoton.2007.89

[8] G. Carpintero et al., "Microwave Photonic Integrated Circuits for Millimeter-Wave Wireless Communications," in Journal of Lightwave Technology, vol. 32, no. 20, pp. 3495-3501, 15 Oct.15, 2014, doi: 10.1109/JLT.2014.2321573.

[9] X. Yu et al., "160 Gbit/s photonics wireless transmission in the 300-500 GHz band", APL Photon., vol. 1, no. 8, 2016.

[10] T. Xu et al., "Bandwidth Compressed Waveform for 60-GHz Millimeter-Wave Radio Over Fiber Experiment," in Journal of Lightwave Technology, vol. 34, no. 14, pp. 3458-3465, 15 July15, 2016, doi: 10.1109/JLT.2016.2565560.

[11] N. Kuse and M. E. Fermann, "Electro-optic comb based real time ultra-high sensitivity phase noise measurement system for high frequency microwaves", Sci. Rep., vol. 7, pp. 2847, Jun. 2017.

[12] S. Pan et al., "Quantum dot mode-locked frequency comb with ultra-stable 25.5 GHz spacing between 20 °C and 120°C", Photonics Res., vol. 8, pp. 1937-1942, 2020. https://doi.org/10.1364/PRJ.399957

[13] V. Torres-Company and A. M. Weiner, "Optical frequency comb technology for ultra-broadband radio-frequency photonics", Laser Photon. Rev., vol. 8, no. 3, pp. 368-393, 2014.

[14] H. H. Elwan, J. Poette and B. Cabon, "Simplified Chromatic Dispersion Model Applied to Ultrawide Optical Spectra for 60 GHz Radio-Over-Fiber Systems," in Journal of Lightwave Technology, vol. 37, no. 19, pp. 5115-5121, 1 Oct.1, 2019, doi: 10.1109/JLT.2019.2929355.

[15] G. Qi et al., "Phase-Noise Analysis of Optically Generated Millimeter-Wave Signals With External Optical Modulation Techniques," in Journal of Lightwave Technology, vol. 24, no. 12, pp. 4861-4875, Dec. 2006, doi: 10.1109/JLT.2006.884990.

[16] H. H. Elwan et al., "Compensation of fiber dispersion induced-power fading in reconfigurable millimeter-wave optical networks", Opt. Commun., vol. 476, no. 126308, pp. 1-7, Dec. 2020, doi: 10.1016/j.optcom.2020.126308

[17] S. Ishimura et al., "Broadband IF-Over-Fiber Transmission With Parallel IM/PM Transmitter Overcoming Dispersion-Induced RF Power Fading for High-Capacity Mobile Fronthaul Links," in IEEE Photonics Journal, vol. 10, no. 1, pp. 1-9, Feb. 2018, Art no. 7900609, doi: 10.1109/JPHOT.2017.2787722.

[18] G.8262. Timing characteristics of a synchronous equipment slave clock https://www.itu.int/rec/T-REC-G.8262-202003-I!Amd1/en

[19] G.8261. Timing and synchronization aspects in packet networks (2008).

[20] R. H. Walden, "Analog-to-digital converter survey and analysis," in IEEE Journal on Selected Areas in Communications, vol. 17, no. 4, pp. 539-550, April 1999, doi: 10.1109/49.761034.